LETTER

doi:10.1038/nature23016

Visible-light-driven methane formation from CO_2 with a molecular iron catalyst

Heng Rao[1], Luciana C. Schmidt[1,2], Julien Bonin[1] & Marc Robert[1]

Converting CO_2 into fuel or chemical feedstock compounds could in principle reduce fossil fuel consumption and climate-changing CO_2 emissions[1,2]. One strategy aims for electrochemical conversions powered by electricity from renewable sources[3–5], but photochemical approaches driven by sunlight are also conceivable[6]. A considerable challenge in both approaches is the development of efficient and selective catalysts, ideally based on cheap and Earth-abundant elements rather than expensive precious metals[7]. Of the molecular photo- and electrocatalysts reported, only a few catalysts are stable and selective for CO_2 reduction; moreover, these catalysts produce primarily CO or HCOOH, and catalysts capable of generating even low to moderate yields of highly reduced hydrocarbons remain rare[8–17]. Here we show that an iron tetraphenylporphyrin complex functionalized with trimethylammonio groups, which is the most efficient and selective molecular electro- catalyst for converting CO_2 to CO known[18–20], can also catalyse the eight-electron reduction of CO_2 to methane upon visible light irradiation at ambient temperature and pressure. We find that the catalytic system, operated in an acetonitrile solution containing a photosensitizer and sacrificial electron donor, operates stably over several days. CO is the main product of the direct CO_2 photoreduction reaction, but a two-pot procedure that first reduces CO_2 and then reduces CO generates methane with a selectivity of up to 82 per cent and a quantum yield (light-to-product efficiency) of 0.18 per cent. However, we anticipate that the operating principles of our system may aid the development of other molecular catalysts for the production of solar fuels from CO_2 under mild conditions.

Iron tetraphenylporphyrins electrochemically reduced to the Fe^0 species have been shown to be the most efficient molecular catalysts for the CO_2-to-CO conversion[18,19]. The nucleophilic Fe centre binds to CO_2 and the Fe–CO_2 adduct is further protonated and reduced to afford CO upon cleavage of one C–O bond. Substitution of the four para-phenyl hydrogens by trimethylammonio groups[18,20] (Fe-p-TMA **1**, Table 1) led to CO formation with selectivity close to 95% in water at pH 7 as well as in aprotic solvent such as N,N-dimethylformamide (DMF), at low overpotentials and with excellent stability (1 day). The fact that the standard redox potential of the Fe^I/Fe^0 is not very negative ($E^0 = -1.50$ V versus SCE in DMF)[20] combined with the high intrinsic activity towards CO_2 reduction makes these catalysts good candidates for photochemical reduction of the gas.

Catalyst **1** was firstly used as a photocatalyst without a photosensitizer under visible light irradiation (wavelength $\lambda > 420$ nm) with triethylamine (TEA, 50 mM) as sacrificial electron donor. Illumination of a 1 atm CO_2-saturated solution of acetonitrile containing 2 μM of **1** at room temperature for 47 h selectively produced CO, with a turnover number in CO relative to catalyst concentration of 33 (entry 1 in Table 1 and Fig. 1a). No side products were observed, and the linear production of CO with time indicates good stability of the catalytic system.

A factor that can potentially limit the catalytic rate of this system[21,22] is the three-electron reduction of the initial Fe^{III} porphyrin species to generate the active Fe^0 state. Using electron donors with high reducing ability should thus be favourable, and adding 0.2 mM of $Ir(ppy)_3$ (**4**, where ppy is phenylpyridine; Table 1) as photosensitizer ($E^0(Ir(ppy)_3^+/Ir(ppy)_3^*) \approx -1.73$ V versus the saturated calomel electrode (SCE) and $E^0(Ir(ppy)_3/Ir(ppy)_3^-) \approx -2.19$ V versus SCE)[23] to the solution indeed enhanced the photocatalytic CO_2 reduction so that 47 h of irradiation gave a turnover number in CO relative to **1** of 198 (entry 2 in Table 1 and Fig. 1b). Adding 0.1 M trifluoroethanol (entry 3 in Table 1) slightly increased the turnover number further to 240, probably owing to trifluoroethanol facilitating the C–O bond cleavage step. With the photosensitizer, products included not only CO but also 10% hydrogen and 12% methane that correspond to turnover numbers of 24 and 31 (entry 2 in Table 1 and Fig. 1b). No other gaseous product was formed, and analysis of the liquid phase failed to detect methanol or formaldehyde by ^{1}H NMR or formate ($HCOO^-$) by ion chromatography. The presence of 0.1 M of trifluoroethanol increased the selectivities (and turnover numbers) for H_2 and CH_4 to 19% (73) and 18% (66), respectively (entry 3 in Table 1 and Fig. 1b). Blank experiments (entries 1 and 5–8 in Table 1) confirmed that no methane is formed in the absence of sensitizer, CO_2, catalyst, electron donor or light.

In isotope labelling experiments conducted under a $^{12}CO_2$ or a $^{13}CO_2$ atmosphere, gas chromatography/mass spectrometry analysis (Fig. 2) identified as reaction product $^{12}CH_4$ (m/z = 16) or $^{13}CH_4$ (m/z = 17), respectively, confirming that methane originates from CO_2 reduction. Increasing the irradiation time increased the amount of CO_2 reduction products generated (Fig. 1c). The longest irradiation time of 102 h produced CO, CH_4 and H_2 with turnover numbers (and selectivities) of 367 (78%), 79 (17%) and 26 (5%), respectively (Table 1, entry 4 and Fig. 1c). These values correspond to a methane production rate of 763 μmol per hour per gram of catalyst (μmol h^{-1} g^{-1}), which exceeds the rate of many other catalysts[12–15,17,24] that generate methane from CO_2. The linear evolution of both CO and CH_4 over more than 80 h and the stable absorption spectrum of the system under irradiation (Extended Data Fig. 1), with no evidence for degradation of the sensitizer **4** or catalyst **1**, illustrate the stability of the catalytic system.

Evolution of the different products (Fig. 1c) shows that methane production starts only after a large amount of CO has built up, suggesting that CO is an intermediate in the methane formation process. We have also previously shown by ultraviolet–visible spectroscopy[22] that irradiation of a CO_2 saturated solution of **1** without a sensitizer (in that case, only CO is obtained) led to the formation of detectable amounts of $Fe^{II}CO$ species. We may thus hypothesize that this iron–carbonyl adduct is an intermediate for further reduction towards methane in the presence of a strong reducing agent. To explore the influence of CO on methane formation more directly, experiments were then conducted in a 1 atm CO-saturated acetonitrile solution under visible light irradiation ($\lambda > 420$ nm), with **4** as sensitizer and TEA as sacrificial electron donor (Fig. 1d). In a 47-h irradiation experiment, this slightly lowered H_2 production and increased CH_4 production by almost a factor of three compared to the experiment using a CO_2-saturated

[1]Université Paris Diderot, Sorbonne Paris Cité, Laboratoire d'Electrochimie Moléculaire, UMR 7591 CNRS, 15 rue Jean-Antoine de Baïf, F-75205 Paris Cedex 13, France. [2]INFIQC-CONICET, Departamento de Química Orgánica, Facultad de Ciencias Químicas, Universidad Nacional de Córdoba, 5000 Córdoba, Argentina.

Table 1 | Catalytic performance and structures of catalysts and sensitizer

1 Fe-p-TMA

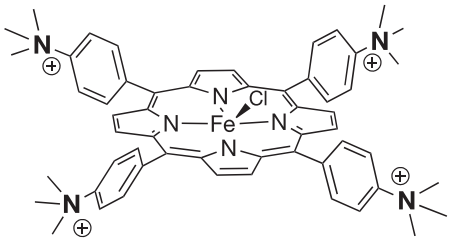

2 Fe-o-OH

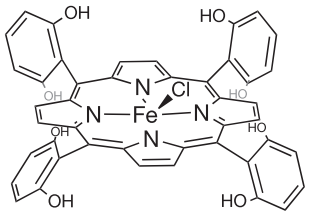

3 FeTPP

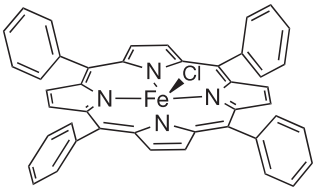

4 $Ir(ppy)_3$

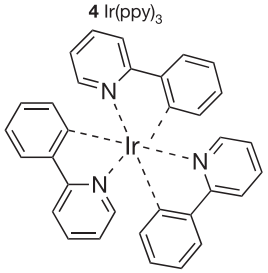

							Turnover numbers		
Entry	[**1**] (μM)	Gas	[**4**] (mM)	[TEA] mM	λ (nm)	Time (h)	CO	CH_4	H_2
1	2	CO_2	-	50	>420	47	33	-	-
2	2	CO_2	0.2	50	>420	47	198	31	24
3*	2	CO_2	0.2	50	>420	47	240	66	73
4	2	CO_2	0.2	50	>420	102	367	79	26
5	2	Ar	0.2	50	>420	47	-	-	43
6	-	CO_2	0.2	50	>420	47	3	-	1
7	2	CO_2	0.2	-	>420	23	5	-	-
8	2	CO_2	0.2	50	Dark	23	-	-	-
9†	2	CO_2	0.2	50	>420	47	139	26	15
10	2	CO	0.2	50	>420	47	-	89	18
11	2	CO	0.2	50	>420	102	-	140	28
12*	2	CO	0.2	50	>420	102	-	159	34
13	-	CO	0.2	50	>420	47	-	-	-
14	2	CO	0.2	50	Dark	23	-	-	-

Summary of the reaction conditions used when evaluating the catalytic performance of catalysts **1** and **2**. Above the table are shown the molecular structures of the iron-based catalysts Fe-p-TMA **1**, Fe-o-OH **2** and FeTPP **3**; and of the visible-light photosensitizer $Ir(ppy)_3$ **4**.
*In the presence of 0.1 M trifluoroethanol.
†Catalyst **2**.

solution: 83% of product was CH_4 and 17% of product was H_2 (entry 10 in Table 1), with the CH_4 formation rate of 1,865 μmol h^{-1} g^{-1}. Blank experiments in the absence of **1** or in the absence of light did not give any reduction product (entries 13 and 14 in Table 1), while a longer irradiation time of 102 h enhanced the selectivity for methane further to 87% (entry 11 in Table 1 and Fig. 1d). Addition of a

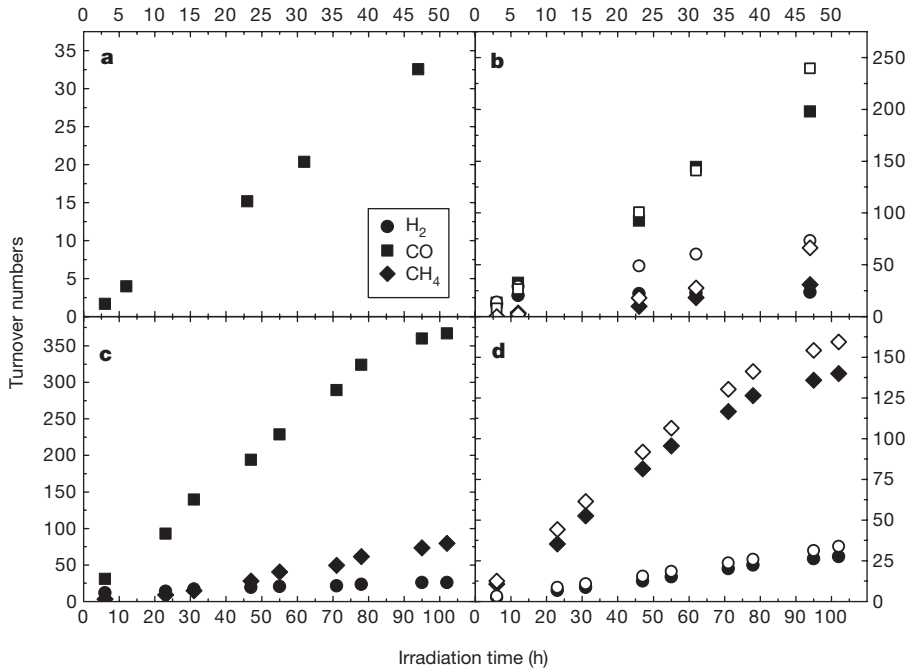

Figure 1 | Photochemical reduction of CO_2 under visible light irradiation. Shown is the formation of gaseous products (in terms of turnover numbers) as a function of irradiation time, using an acetonitrile solution saturated with 1 atm CO_2 (**a**, **b**, **c**) or 1 atm CO (**d**) and containing 2 μM of catalyst **1** and 50 mM of TEA. **a**, With no sensitizer, only CO is produced. **b**, When 0.2 mM of sensitizer **4** is present, H_2, CO and CH_4 are produced (filled symbols); adding 0.1 M of trifluoroethanol increases their production rate (open symbols). **c**, H_2, CO and CH_4 product evolution over an extended irradiation time in the presence of 0.2 mM of **4**. **d**, Under a CO atmosphere and with 0.2 mM of sensitizer **4** present, H_2 and CH_4 are produced (filled symbols); adding 0.1 M of trifluoroethanol increases their production rate (open symbols). Data points are the results of at least two individual experiments and typical uncertainty on turnover numbers is about 5%, corresponding to the size of the data points. Source data for this figure is available in the online version of the paper.

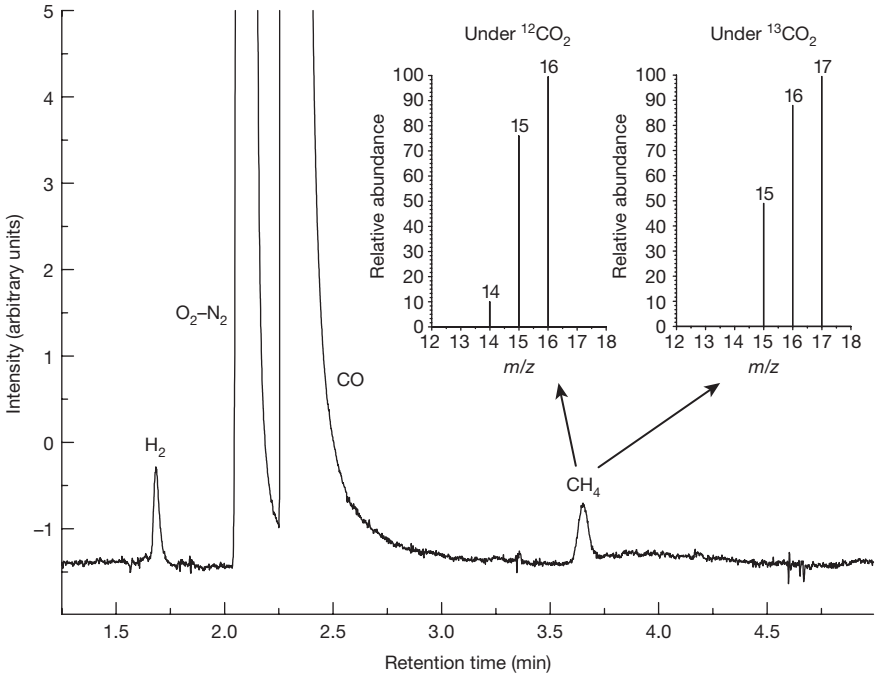

Figure 2 | Methane detection. Typical gas chromatogram observed during long-term irradiation of a solution containing 2 μM of catalyst **1**, 50 mM of TEA and 0.2 mM of sensitizer **4**, under $^{12}CO_2$ or $^{13}CO_2$ atmosphere. The inset shows the mass spectra of methane generated under a $^{12}CO_2$ or $^{13}CO_2$ atmosphere.

weak acid in moderate concentration (trifluoroethanol 0.1 M) slightly increased the methane formation rate (from a turnover number of 140 to 159) with some loss of selectivity (from 87% to 82%; entry 12 in Table 1). The successful methane evolution under these conditions over 102 h with an average rate of 1,467 μmol h^{-1} g^{-1} illustrate the robustness, activity and selectivity of the catalytic system.

When replacing catalyst **1** by Fe-o-OH (**2**, Table 1), which carries –OH groups at all ortho, ortho′ positions of the four phenyl rings[25] instead of trimethylammonio groups at the para positions, methane was also evolved although in slightly smaller amounts (turnover number 26 after 47 h irradiation and 14% selectivity, Table 1, entry 9). The standard redox potential $E^0(Fe^I/Fe^0) = -1.575$ V versus SCE[26] in DMF for catalyst **2** is only 75 mV more negative than for **1**, and as in the latter case, the substituents on the phenyls may help stabilizing reaction intermediates (through internal H bonds involving the –OH groups). In contrast, the non-substituted tetraphenyl Fe porphyrin (FeTPP **3**, Table 1) only gives CO and H_2 (with turnover numbers/selectivities of 84/79% and 22/21%, respectively) under the same irradiation conditions[27], probably owing to its much more negative standard redox potentials (for example, $E^0(Fe^I/Fe^0) = -1.67$ V versus SCE in DMF)[28] and the absence of phenyl ring substituents for stabilizing intermediate species involved in hydrocarbon production. The ability to produce methane is thus not restricted to catalyst **1**, but is probably a more general property of Fe porphyrins that have a sufficiently positive standard redox potential and are functionalized with substituents that can stabilize intermediates involved in the catalytic cycle.

Another key parameter for CO_2 reduction beyond the two-electron production of CO is the driving force for charge transfer from the excited state of the sensitizer. When replacing **4** by the less-reducing ruthenium complex $Ru(bpy)_3^{2+}$ (where bpy is 2,2′-bipyridine; $E^0(Ru(bpy)_3^{2+}/Ru(bpy)_3^{+}) \approx -1.33$ V versus SCE and $E^0(Ru(bpy)_3^{3+}/Ru(bpy)_3^{2+*}) = -0.81$ V versus SCE)[23], only CO and H_2 and no CH_4 were obtained, possibly because the Ru excited state or its reduced form are not able to trigger the carbonyl reduction from the $Fe^{II}CO$ adduct. Emission quenching experiments between the excited state of the sensitizer **4*** and **1** on one hand and **4*** and TEA on the other hand revealed very weak quenching with TEA, while it is very efficient and diffusion-controlled with **1** ($k_q \approx 1.7 \times 10^{10}$ M^{-1} s^{-1}, Extended Data Fig. 2), suggesting that direct electron transfer occurs from the excited sensitizer **4*** to the Fe porphyrin. This is in line with the standard redox potential value of the excited iridium complex ($E^0(\mathbf{4}^+/\mathbf{4}^*) \approx -1.73$ V versus SCE), which is more negative than all three redox couples related to the Fe porphyrin (Fe^{III}/Fe^{II}, Fe^{II}/Fe^{I} and Fe^{I}/Fe^{0}). After electron transfer, the oxidized $\mathbf{4}^+$ is reduced by the sacrificial electron donor TEA upon irradiation, thereby closing the catalytic cycle and generating the protonated triethylamine $TEAH^+$ that could then act as proton donor, as seen before[27]. Figure 3 sketches a plausible mechanism based on these considerations, which involves a postulated formyl intermediate[29,30] that may be stabilized by through-space interactions between the positive charges of the trimethylammonio groups and the partial negative charge on the CHO species bound to the metal. With complete reduction of the $Fe^{II}CO$ adduct necessitating six electrons, the quantum yield for CH_4 formation is $\Phi = 0.18\%$ (see Methods).

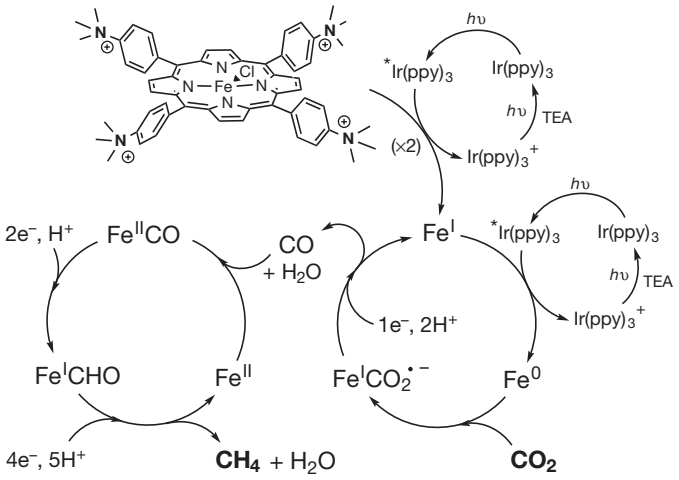

Figure 3 | Sketch of the proposed mechanism for CO_2 reduction to CH_4 by catalyst 1. Initially, the starting Fe^{III} porphyrin (top left) is reduced with three electrons to the catalytically active Fe^0 species. The Fe^0 species reduces CO_2, with the resultant Fe^I regenerated through electron transfer from the excited photosensitizer (right-hand side cycle). The CO produced binds to Fe^{II} and is further reduced with a total of six electrons (transferred from the excited sensitizer) and six protons to generate methane, via a postulated Fe^I-formyl (Fe^ICHO) intermediate (left-hand side cycle). For more detailed discussion, see text. *hυ*, light irradiation.

We anticipate that further spectroscopic investigation, in conjunction with quantum calculations, will help decipher in greater detail the reduction mechanism at play. This insight should aid the development of more efficient catalytic systems that make use of Earth-abundant Fe-based molecular complexes to reduce CO_2 into CO and then into CH_4 under mild conditions and driven by visible light.

Online Content Methods, along with any additional Extended Data display items and Source Data, are available in the online version of the paper; references unique to these sections appear only in the online paper.

Received 6 January; accepted 6 June 2017.
Published online 17 July 2017.

1. Jhong, H.-R. M., Ma, S. & Kenis, P. J. A. Electrochemical conversion of CO_2 to useful chemicals: current status, remaining challenges, and future opportunities. *Curr. Opin. Chem. Eng.* **2,** 191–199 (2013).
2. Aresta, M., Dibenedetto, A. & Angelini, A. Catalysis for the valorization of exhaust carbon: from CO_2 to chemicals, materials, and fuels. Technological use of CO_2. *Chem. Rev.* **114,** 1709–1742 (2014).
3. Qiao, J., Liu, Y., Hong, F. & Zhang, J. A review of catalysts for the electroreduction of carbon dioxide to produce low-carbon fuels. *Chem. Soc. Rev.* **43,** 631–675 (2014).
4. Parajuli, R. *et al.* Integration of anodic and cathodic catalysts of Earth-abundant materials for efficient, scalable CO_2 reduction. *Top. Catal.* **58,** 57–66 (2015).
5. Tatin, A. *et al.* Efficient electrolyzer for CO_2 splitting in neutral water using Earth-abundant materials. *Proc. Natl Acad. Sci. USA* **113,** 5526–5529 (2016).
6. Sahara, G. & Ishitani, O. Efficient photocatalysts for CO_2 reduction. *Inorg. Chem.* **54,** 5096–5104 (2015).
7. Takeda, H., Cometto, C., Ishitani, O. & Robert, M. Electrons, photons, protons and Earth-abundant metal complexes for molecular catalysis of CO_2 reduction. *ACS Catal.* **7,** 70–88 (2017).
8. Shen, J. *et al.* Electrocatalytic reduction of carbon dioxide to carbon monoxide and methane at an immobilized cobalt protoporphyrin. *Nat. Commun.* **6,** 8177 (2015).
9. Weng, Z. *et al.* Electrochemical CO_2 reduction to hydrocarbons on a heterogeneous molecular Cu catalyst in aqueous solution. *J. Am. Chem. Soc.* **138,** 8076–8079 (2016).
10. Manthiram, K., Beberwyck, B. J. & Alivisatos, A. P. Enhanced electrochemical methanation of carbon dioxide with a dispersible nanoscale copper catalyst. *J. Am. Chem. Soc.* **136,** 13319–13325 (2014).
11. Xie, M. S. *et al.* Amino acid modified copper electrodes for the enhanced selective electroreduction of carbon dioxide towards hydrocarbons. *Energy Environ. Sci.* **9,** 1687–1695 (2016).
12. Wu, T. *et al.* A carbon-based photocatalyst efficiently converts CO_2 to CH_4 and C_2H_2 under visible light. *Green Chem.* **16,** 2142–2146 (2014).
13. AlOtaibi, B., Fan, S., Wang, D., Ye, J. & Mi, Z. Wafer-level artificial photosynthesis for CO_2 reduction into CH_4 and CO using GaN nanowires. *ACS Catal.* **5,** 5342–5348 (2015).
14. Liu, X., Inagaki, S. & Gong, J. Heterogeneous molecular systems for photocatalytic CO_2 reduction with water oxidation. *Angew. Chem. Int. Ed.* **55,** 14924–14950 (2016).
15. Wang, Y. *et al.* Facile one-step synthesis of hybrid graphitic carbon nitride and carbon composites as high-performance catalysts for CO_2 photocatalytic conversion. *ACS Appl. Mater. Interf.* **8,** 17212–17219 (2016).
16. Zhu, S. *et al.* Photocatalytic reduction of CO_2 with H_2O to CH_4 over ultrathin $SnNb_2O_6$ 2D nanosheets under visible light irradiation. *Green Chem.* **18,** 1355–1363 (2016).
17. Yu, L. *et al.* Enhanced activity and stability of carbon-decorated cuprous oxide mesoporous nanorods for CO_2 reduction in artificial photosynthesis. *ACS Catal.* **6,** 6444–6454 (2016).
18. Azcarate, I., Costentin, C., Robert, M. & Savéant, J.-M. A study of through-space charge interaction substituent effects in molecular catalysis leading to the design of the most efficient catalyst of CO_2-to-CO electrochemical conversion. *J. Am. Chem. Soc.* **138,** 16639–16644 (2016).
19. Bonin, J., Maurin, A. & Robert, M. Molecular catalysis of the electrochemical and photochemical reduction of CO_2 with Fe and Co metal based complexes. Recent advances. *Coord. Chem. Rev.* **334,** 184–198 (2017).
20. Costentin, C., Robert, M., Savéant, J.-M. & Tatin, A. Efficient and selective molecular catalyst for the CO_2-to-CO electrochemical conversion in water. *Proc. Natl Acad. Sci. USA* **112,** 6882–6886 (2015).
21. Bonin, J., Robert, M. & Routier, M. Selective and efficient photocatalytic CO_2 reduction to CO using visible light and an iron-based homogeneous catalyst. *J. Am. Chem. Soc.* **136,** 16768–16771 (2014).
22. Rao, H., Bonin, J. & Robert, M. Non-sensitized selective photochemical reduction of CO_2 to CO under visible light with an iron molecular catalyst. *Chem. Commun.* **53,** 2830–2833 (2017).
23. Prier, C. K., Rankic, D. A. & MacMillan, D. W. C. Visible light photoredox catalysis with transition metal complexes: applications in organic synthesis. *Chem. Rev.* **113,** 5322–5363 (2013).
24. Wang, H., Chen, Y., Hou, X., Ma, C. & Tan, T. Nitrogen-doped graphenes as efficient electrocatalysts for the selective reduction of carbon dioxide to formate in aqueous solution. *Green Chem.* **18,** 3250–3256 (2016).
25. Costentin, C., Drouet, S., Robert, M. & Savéant, J.-M. A local proton source enhances CO_2 electroreduction to CO by a molecular Fe catalyst. *Science* **338,** 90–94 (2012).
26. Costentin, C., Passard, G., Robert, M. & Savéant, J.-M. Pendant acid-base groups in molecular catalysts: H-bond promoters or proton relays? Mechanisms of the conversion of CO_2 to CO by electrogenerated iron(0) porphyrins bearing prepositioned phenol functionalities. *J. Am. Chem. Soc.* **136,** 11821–11829 (2014).
27. Bonin, J., Chaussemier, M., Robert, M. & Routier, M. Homogeneous photocatalytic reduction of CO_2 to CO using iron(0) porphyrin catalysts: mechanism and intrinsic limitations. *ChemCatChem* **6,** 3200–3207 (2014).
28. Bhugun, I., Lexa, D. & Savéant, J.-M. Homogeneous catalysis of electrochemical hydrogen evolution by iron(0) porphyrins. *J. Am. Chem. Soc.* **118,** 3982–3983 (1996).
29. Appel, A. M. *et al.* Frontiers, opportunities, and challenges in biochemical and chemical catalysis of CO_2 fixation. *Chem. Rev.* **113,** 6621–6658 (2013).
30. Davies, S. G., Hibberd, J. & Simpson, S. J. Disproportionation of the iron carbonyl hydride (n^5-C_5H_5)Fe(CO)H($Ph_2PCH_2CH_2PPh_2$) to the iron methyl (n^5-C_5H_5)Fe($Ph_2PCH_2CH_2PPh_2$)Me. *J. Chem. Soc. Chem. Commun.*1404–1405 (1982).

Acknowledgements This work was partially supported by the CNRS, Défi Transition énergétique "Emergence CO_2" (the PERIODIC project). H.R. thanks the China Scholarship Council for a PhD fellowship (CSC student number 201507040033). We thank D. Clainquart (Université Paris Diderot) for assistance in gas chromatography/mass spectrometry analysis and I. Azcarate for porphyrin synthesis.

Author Contributions M.R. conceived the research, J.B. and M.R. directed the project and co-wrote the paper. J.B. conceived the experimental setup. J.B., L.C.S. and H.R. conducted experiments. H.R., J.B. and M.R. analysed results. All the authors contributed to the scientific interpretation and reviewed the manuscript.

Author Information Reprints and permissions information is available at www.nature.com/reprints. The authors declare no competing financial interests. Readers are welcome to comment on the online version of the paper. Publisher's note: Springer Nature remains neutral with regard to jurisdictional claims in published maps and institutional affiliations. Correspondence and requests for materials should be addressed to J.B. (julien.bonin@univ-paris-diderot.fr) and M.R. (robert@univ-paris-diderot.fr).

METHODS

Synthesis of catalysts 1 and 2. The synthesis of chloro iron(III) 5,10,15,20-tetra(40-N,N,N-trimethylanilinium)porphyrin (Fe-p-TMA, **1**)[20] and chloro iron(III) 5,10,15,20-tetrakis(2′,6′-dihydroxyphenyl) porphyrin (Fe-o-OH, **2**)[25] have been described elsewhere.

Photochemical measurements. Irradiations of acetonitrile (99.9% extra-dry, Acros Organics) solutions containing triethylamine (99% pure, Acros Organics) as sacrificial electron donor, and *fac*-(tris-(2-phenylpyridine))iridium(III) ($Ir(ppy)_3$, **4**; 99%, Aldrich) as sensitizer were realized in a closed 1 cm × 1 cm quartz suprasil cuvette (Hellma 117.100F-QS) equipped with home-designed headspace glassware. Solutions were saturated with argon (>99.998%, Air Liquide), $^{12}CO_2$ (>99.7%, Air Liquide), $^{13}CO_2$ (99 atom% ^{13}C, Aldrich) or ^{12}CO (> 99.997%, Air Liquide) for 20 min before irradiation. A Newport LCS-100 solar simulator, equipped with an AM1.5 G standard filter allowing 1 Sun irradiance, was used as the light source combined with a Schott GG420 longpass filter and 2-cm-long glass (OS) cell filled with deionized water to prevent catalyst absorbance and to cut off infrared and low ultraviolet.

Spectrophotometric measurements. Ultraviolet–visible absorption data were collected with an Analytik Jena Specord 600 ultraviolet–visible spectrophotometer. Emission quenching measurements were conducted with a Cary Eclipse fluorescence spectrophotometer (Agilent Technologies), with the excitation wavelength set at 420 nm and the emission spectrum measured between 430 nm and 700 nm. Emission intensities used for the Stern–Volmer analysis were taken at 517 nm, that is, the emission maximum of **4**. The lifetime of the emissive excited state of **4** was taken as 1.9 μs, as reported before[31].

Reduction products analysis. Gaseous products analysis was performed with an Agilent Technology 7820A gas chromatography system equipped with a capillary column (CarboPLOT P7, length 25 m, inner diameter 25 mm) and a thermal conductivity detector. Calibration curves for H_2, CO and CH_4 were established separately. Control experiments, with no catalyst, no CO_2 or no light were conducted under the same conditions otherwise as the full system. Ionic chromatography measurements were performed with a Thermo Scientific Dionex ICS-1100 system. Mass spectra were obtained by a ThermoFisher Scientific TRACE Ultra gas chromatograph equipped with a CP 7514 column (Agilent Technologies) and coupled to a DSQ II mass spectrometer in positive ionization mode, using a TriPlus headspace autosampler.

Turnover number calculation. Turnover number is practically defined as the number of catalytic cycles per catalyst amount. The number of moles of H_2, CO and CH_4 was determined by converting peak integrations from gas chromatography measurements into moles in the sample headspace by using individual calibration curves and taking into account the irradiated sample volume (3.5 ml).

Quantum yield calculation. The number of incident photons was measured using the classical iron ferrioxalate ($K_3Fe(C_2O_4)_3$) chemical actinometer, following the procedure reported previously[32] and using known parameters for calculations[33]. Using three independent measurements, we determined that the number of incident photons to the sample was $(2.18 \pm 0.17) \times 10^{19}$ photons per hour. The CO-to-CH_4 reduction being a six-electron process, the overall quantum yield Φ of the process was determined using the following equation:

$$\Phi_{CH_4}\,(\%) = \frac{\text{Number of } CH_4 \text{ molecules formed} \times 6}{\text{Number of incident photons}} \times 100$$

Taking 159 as the highest turnover number for CH_4 (Table 1, entry 12), we obtain a quantum yield Φ of about 0.18% after 102 h of irradiation.

Data availability. The data that support the findings of this study are available from the corresponding authors upon reasonable request. Original experimental data that support the findings of this study are available from the corresponding authors upon reasonable request. Source data for Fig. 1 is available in the online version of the paper.

31. Dedeian, K., Djurovich, P. I., Garces, F. O., Carlson, G. & Watts, R. J. A new synthetic route to the preparation of a series of strong photoreducing agents: *fac*-tris-ortho-metalated complexes of iridium(III) with substituted 2-phenylpyridines. *Inorg. Chem.* **30,** 1685–1687 (1991).
32. Alsabeh, P. G. *et al.* Iron-catalyzed photoreduction of carbon dioxide to synthesis gas. *Catal. Sci. Technol.* **6,** 3623–3630 (2016).
33. Montalti, M., Credi, A., Prodi, L & Gandolfi, M. T. *Handbook of Photochemistry* 3rd edn (CRC Press, 2006).

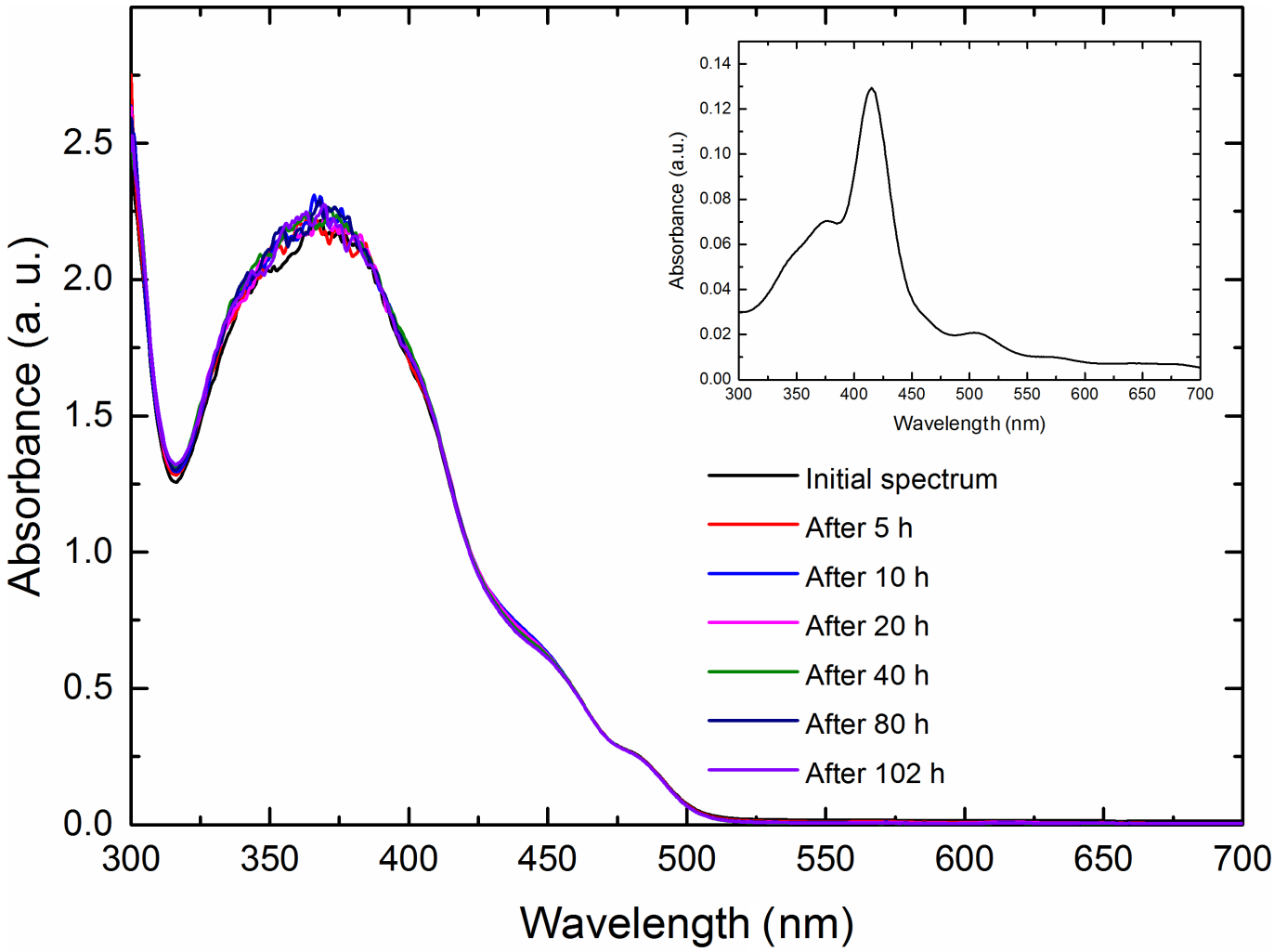

Extended Data Figure 1 | Evolution of the absorption spectrum with time. The absorption spectrum of a CO_2-saturated acetonitrile solution containing 2 μM of **1**, 0.2 mM of **4**, 0.05 M of TEA upon visible (>420 nm) light irradiation remains stable over the course of experiments, highlighting the stability of the system. The inset shows the absorption spectrum of 2 μM of catalyst **1** in acetonitrile (no sensitizer **4**), revealing that in the photocatalytic mix, >90% of photons above 420 nm are absorbed by **4**.

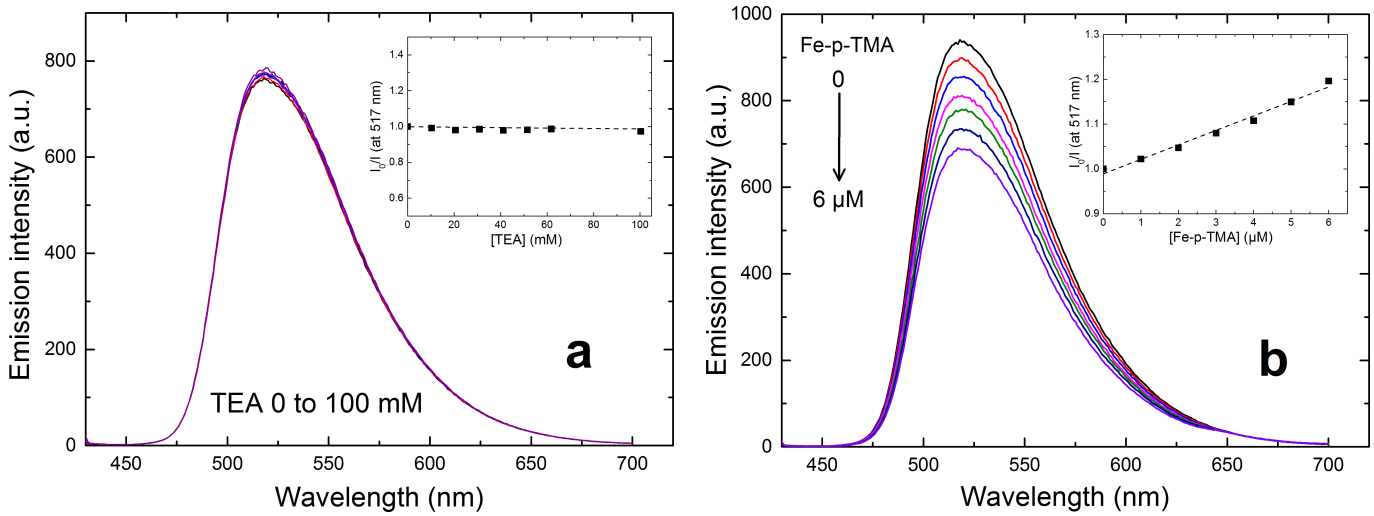

Extended Data Figure 2 | Sensitizer 4 emission quenching after excitation at 420 nm. a, Upon increasing concentration of TEA in a 0.1 mM acetonitrile solution of **4**, no emission quenching is observed, as confirmed by the Stern–Volmer analysis (inset). **b**, Upon increasing concentration of **1** in a 0.2 mM acetonitrile solution of **4**, emission quenching is observed corresponding to a diffusion-controlled quenching rate of $(1.7 \pm 0.1) \times 10^{10}\ M^{-1}\ s^{-1}$ as determined by Stern–Volmer analysis (inset). a.u., arbitrary units. I_0/I is the emission intensity without quencher divided by the emission intensity with a known concentration of quencher.